# Relation of myocardial oxygen consumption and function to high energy phosphate utilization during graded hypoxia and reoxygenation in sheep in vivo.

M A Portman, … , T A Standaert, X H Ning

*J Clin Invest.* 1995;95(5):2134-2142. https://doi.org/10.1172/JCI117902.

**Research Article**

This study investigates the relation between myocardial oxygen consumption (MVO2), function, and high energy phosphates during severe hypoxia and reoxygenation in sheep in vivo. Graded hypoxia was performed in open-chested sheep to adjust PO2 to values where rapid depletion of energy stores occurred. Highly time-resolved 31P nuclear magnetic resonance spectroscopy enabled monitoring of myocardial phosphates throughout hypoxia and recovery with simultaneous MVO2 measurement. Sheep undergoing graded hypoxia (n = 5) with an arterial PO2 nadir of 13.4 +/- 0.5 mmHg, demonstrated maintained rates of oxygen consumption with large changes in coronary flow as phosphocreatine (PCr) decreased within 4 min to 40 +/- 7% of baseline. ATP utilization rate increased simultaneously 59 +/- 20%. Recovery was accompanied by marked increases in MVO2 from 2.0 +/- 0.5 to 7.2 +/- 1.9 mumol/g per min, while PCr recovery rate was 4.3 +/- 0.6 mumol/g per min. ATP decreased to 75 +/- 6% of baseline during severe hypoxia and did not recover. Sheep (n = 5) which underwent moderate hypoxia (PO2 maintained 25-35 mmHg for 10 min) did not demonstrate change in PCr or ATP. Functional and work assessment (n = 4) revealed that cardiac power increased during the graded hypoxia and was maintained through early reoxygenation. These studies show that (a) MVO2 does not decrease during oxygen deprivation in vivo despite marked and […]



# Relation of Myocardial Oxygen Consumption and Function to High Energy Phosphate Utilization during Graded Hypoxia and Reoxygenation in Sheep In Vivo

**Michael A. Portman, Thomas A. Standaert, and Xue-Han Ning**
*Division of Cardiology, Department of Pediatrics, University of Washington and Children's Hospital and Medical Center of Seattle, Seattle, Washington 98195*

## Abstract

**This study investigates the relation between myocardial oxygen consumption ($MV_{O_2}$), function, and high energy phosphates during severe hypoxia and reoxygenation in sheep in vivo. Graded hypoxia was performed in open-chested sheep to adjust $P_{O_2}$ to values where rapid depletion of energy stores occurred. Highly time-resolved $^{31}P$ nuclear magnetic resonance spectroscopy enabled monitoring of myocardial phosphates throughout hypoxia and recovery with simultaneous $MV_{O_2}$ measurement. Sheep undergoing graded hypoxia ($n = 5$) with an arterial $P_{O_2}$ nadir of 13.4±0.5 mmHg, demonstrated maintained rates of oxygen consumption with large changes in coronary flow as phosphocreatine (PCr) decreased within 4 min to 40±7% of baseline. ATP utilization rate increased simultaneously 59±20%. Recovery was accompanied by marked increases in $MV_{O_2}$ from 2.0±0.5 to 7.2±1.9 μmol/g per min, while PCr recovery rate was 4.3±0.6 μmol/g per min. ATP decreased to 75±6% of baseline during severe hypoxia and did not recover. Sheep ($n = 5$) which underwent moderate hypoxia ($P_{O_2}$ maintained 25–35 mmHg for 10 min) did not demonstrate change in PCr or ATP. Functional and work assessment ($n = 4$) revealed that cardiac power increased during the graded hypoxia and was maintained through early reoxygenation. These studies show that (*a*) $MV_{O_2}$ does not decrease during oxygen deprivation in vivo despite marked and rapid decreases in high energy phosphates; (*b*) contractile function during hypoxia in vivo does not decrease during periods of PCr depletion and intracellular phosphate accumulation, and this may be related to marked increases in circulating catecholamines during global hypoxia. The measured creatine rephosphorylation rate is 34±11% of predicted ($P < 0.01$) calculated from reoxygenation parameters, which indicates that some mitochondrial respiratory uncoupling also occurs during the rephosphorylation period. (*J. Clin. Invest.* 1995. 95:2134–2142.) Key words: ATP • phosphocreatine • oxidative phosphorylation • mitochondria • nuclear magnetic resonance**

## Introduction

Severe hypoxia ultimately leads to contractile failure, which is attributed to an imbalance between myocardial oxygen supply and demand (1–4). Sudden extreme oxygen deprivation causes rapid depletion of energy stores in the form of the high energy phosphates, phosphocreatine, and ATP, as well as accumulation of ATP hydrolysis products. In isolated myocytes (5) and buffer-perfused hearts (5, 6) anoxia or hypoxia results in a reduced oxidative phosphorylation rate. Myocardial respiration wanes despite increasing ADP and intracellular phosphate (Pi),[1] which both stimulate mitochondrial ATP production under aerobic conditions. The intact animal generally maintains or increases myocardial oxygen consumption during early or moderate hypoxia (7–9). Small decreases in myocardial phosphocreatine content with no depletion of the cytosolic ATP pool have been documented during moderate hypoxic conditions (10, 11). However, myocardial oxygen consumption rates have not been directly measured during periods of rapid high energy phosphate depletion and repletion in the intact animal. The purpose of this study was to examine the relation between myocardial oxygen consumption, function, and high energy phosphates during severe hypoxia and reoxygenation in vivo. Additionally, rephosphorylation parameters were measured to determine if evidence of respiratory uncoupling or mitochondrial damage occurs during reoxygenation in vivo. Graded hypoxia was performed in an effort to gradually reduce arterial oxygen tension to attain the $P_{O_2}$ at which high energy phosphate stores rapidly decreased. Highly time-resolved $^{31}P$ nuclear magnetic resonance (NMR) spectroscopy enabled monitoring of myocardial phosphates throughout hypoxia and recovery with simultaneous measurement of oxygen consumption. Consequently, these measurements enhanced analysis of mitochondrial function in vivo during reoxygenation.

## Methods

Animal preparation. Animals used in this study were handled in accordance with institutional and National Institutes of Health animal care and use guideline. Sheep between 30 and 70 d old (mean 47 d±6.8) were sedated with an intramuscular injection of 10 mg/kg ketamine, and 0.2–0.4 mg/kg xylazine, intubated, and then ventilated (C-900 pediatric ventilator; Siemens Corp., Schaumberg, IL) with room air and oxygen, followed by an intravenous dose of alpha-chloralose (40 mg/kg). Femoral arterial cannulation was performed for monitoring systemic blood pressure and sampling blood. Arterial pH was maintained between 7.35 and 7.45 by adjustment of ventilatory tidal volume and

Address correspondence to Michael A. Portman, Department of Pediatrics RD-20, University of Washington, Seattle, WA 98195. Phone: 206-685-7186; FAX: 206-543-3184.

*Received for publication 25 October 1994 and in revised form 16 December 1994.*

J. Clin. Invest.

0021-9738/95/05/2134/09 $2.00
Volume 95, May 1995, 2134–2142

1. *Abbreviations used in this paper:* $FIO_2$, fractional inspiratory oxygen tension; NMR, nuclear magnetic resonance; PCr, phosphocreatine; $pH_i$, intracellular pH; Pi, intracellular phosphate.

correction of metabolic acidosis with sodium bicarbonate infusion. After a median sternotomy, the pericardial fat pad was exposed and removed. Platinum-tipped pacing electrodes were sutured to the right atrial appendage. Coronary sinus flow was measured as previously described, via an extracorporeal shunt between the coronary sinus and the superior vena cava, fashioned by cannulating both jugular veins with heparin flushed tubing (Tygon; Norton Performance Plastics Corp., Akron, OH, $^1/_8$-inch internal diameter, $^3/_{16}$-inch OD) (12). One tube end was advanced retrograde into the coronary sinus, while the other was positioned in the superior vena cava. A cannulating ultrasonic transit time probe was inserted in the tubing for continuous measurement of shunt flow, as was a T connector for sampling $O_2$ content. The sinus catheter tip was positioned between the coronary sinus orifice and the juncture of the great cardiac and hemizygous veins. A suture was placed around the coronary sinus to anchor the tip and direct all coronary sinus drainage into the Tygon shunt. The hemizygous vein, which drains directly into the coronary sinus in sheep, was then ligated. The flow monitoring system provided digital display and continuous hard copy tracing. A 2-cm diameter round NMR surface coil was sutured to the pericardium overlying the left ventricle. The flexibility of the coil allowed unrestricted cardiac movement and filling, while keeping the coil in reproducible proximity to the heart. The thoracotomy opening was then sealed with plastic wrap to prevent water loss. The lamb was wrapped in a water-circulating heating blanket that maintained body core temperature at ~ 38°C, and placed in a Lucite cradle which fit into the 26-cm clear bore of the 4.7 Tesla Chemical Shift Imager (General Electric Co., Fremont, CA) system. The surface coil was positioned at the magnetic center of the system.

*NMR measurements.* After transfer of the lamb into the magnet, the NMR surface coil was tuned to 81 MHz and matched to 50 ohms. Respiration was maintained within the magnet via 8 ft of tubing attached to the expiratory and inspiratory ports of the ventilator. Blood pressure was monitored using a solid state nonmagnetic pressure transducer (Cobe Lab Inc., Lakewood, CO) positioned just outside the magnet bore.

NMR data were collected with a spectrometer (General Electric Co.) using GE-resident OMEGA software. Shimming on the $^1$H-free-induction decay at 200 MHz and acquisition of $^{31}$P spectra were performed as previously described using both cardiac and respiratory gating (13), during which the heart is atrially paced at a rate equivalent to the lowest respiratory harmonic above the intrinsic sinus rate. Interpulse delay was ~ 2 s as determined by the respiratory cycle. The pulse width which optimized the phosphocreatine (PCr) signal was chosen for each study and was between 15 and 25 $\mu$s. All spectra were obtained using a simple one pulse sequence. Data were acquired with a 5,000-Hz sweep width and 2,000 data points. 15 spectra (30 s) were stored in each block and four consecutive acquisition blocks were averaged for some analyses. All spectra were analyzed using a least squares fitting program (14). Before each protocol, blocks of 120 acquisitions were obtained for reference use in the least squares analysis program. Intracellular pH was determined from the chemical shift difference Pi-PCr as previously described. Although the peaks from 2,3 diphosphoglycerate frequently contaminate the Pi peak in heart spectra from several species, this does not occur in sheep (13).

*Graded hypoxia (group A).* After stabilization, inspiratory oxygen concentration was adjusted to 21–22%. Baseline data were obtained for 8 min, followed by a decrease in fractional inspiratory oxygen concentration ($FIo_2$) by 3% increments every 4 min. This graded hypoxia protocol was continued until 4 min at $FIo_2$ 3% was completed. The animal was then ventilated with 100% oxygen and data collected for an additional 16 min. During each 4-min period, coronary sinus and arterial samples were obtained for blood gases (Corning Inc., Corning, NY) and hemoglobin saturation (Radiometer OSM2; Radiometer America Inc., Westlake, OH). Samples were centrifuged and serum frozen (−70°C) prior to determination of glucose and lactate content. NMR data were collected simultaneously ($n$ = 5).

*Steady state hypoxia (group B).* After the stabilization period, the inspiratory oxygen concentration was adjusted to 6–9% for 18 min, the same length of time as the graded hypoxia protocol ($n$ = 3). Blood samples were obtained similarly every 4 min, and $Po_2$ maintained between 25 and 35 mmHg during the hypoxic period. Recovery was performed as in the graded hypoxia protocol. NMR data were collected as in group A.

*Cardiac pacing.* Pacing was maintained throughout the protocols and adjusted upwards to the next respiratory harmonic as soon as intrinsic sinus competition with pacing became apparent. During recovery pacing was intermittently discontinued for a few seconds to determine intrinsic heart rate, and then pacing readjusted to a lower harmonic of the respiratory rate if appropriate.

*Cardiac function studies (group C).* In a separate group of animals ($n$ = 4), the surgical procedure was altered. A transit time flow probe was place around the aorta, just distal to the aortic valve. Additionally, a 2-cm length catheter was inserted through the left ventricular apex, and attached to a pressure transducer. Cardiac work and hemodynamic parameters including left ventricular systolic pressure, end diastolic pressure, dP/dt, and left ventricular power were then measured in these animals. Due to technical limitations, placements of the coronary sinus shunt and NMR surface coil were not performed in this group; oxygen consumption and NMR data were then not collected. Before initiation of the graded hypoxia protocol, function studies were performed at a various pacing rates analogous to the respiratory harmonic rates used in group A and B. This provided a basis for comparison of dP/dt, which is a heart rate–dependent value, and may change somewhat during hypoxia. The protocol was then initiated at the respiratory harmonic above the intrinsic sinus rate. Serum catecholamine levels were obtained from this group during the stabilization period, at $FIo_2$ 21%, and at $FIo_2$ 3%. Catecholamines were analyzed using standard HPLC techniques (Bio-Rad Instruction Manual 195-6051, Plasma Catecholamines by HPLC; BioRad Laboratories, Hercules CA).

*Myocardial oxygen consumption.* Oxygen content was determined using dissolved oxygen calculated from the $Po_2$ and oxyhemoglobin determined from hemoglobin content and saturation available from the OSM2. $MVo_2$ was calculated from the coronary arteriovenous difference times coronary sinus flow rate.

*Substrate analysis.* Glucose and lactate were determined spectrophotometrically using an analyzer (GM7; Analox Instruments Ltd., London, United Kingdom).

*Statistical analyses.* All animals served as their own controls. Data were analyzed using ANOVA. Paired $t$ test analysis was used when appropriate. All PCr and ATP data are reported relative to peak areas at 21% $FIo_2$. All descriptive data are reported as means±SE.

## Results

A summary of hemodynamic and blood gas parameters for sheep, which underwent the graded hypoxia protocol during simultaneous acquisition of NMR data are presented in Table I. A steady decrease in arterial $Po_2$ and arterial oxygen content occurred during this protocol with a significant drop in coronary sinus $Po_2$ at an $FIo_2$ of 6%. Changes in coronary sinus flow are illustrated in Fig. 1. The largest increase occurred at $FIo_2$ 3% (mean arterial $Po_2$ 13.4±0.5). Myocardial oxygen consumption (Fig. 2) as well as coronary oxygen delivery was maintained through all periods of hypoxia. Both increased substantially during the initial reoxygenation period, followed by a decline to control levels after the first 4 min of recovery.

Lactate production is frequently considered to be a gauge of anaerobic metabolism. Net lactate uptake predominates in the aerobically functioning sheep heart, as this substrate is converted to pyruvate and oxidized (15). In this study, net lactate uptake continues through the protocol until $FIo_2$ drops to 6% (Fig. 3) indicating that an increase in anaerobic glycolytic metabolism has transpired. Net lactate release occurs despite the

*Table I. $PO_2$ and Hemodynamic Parameters during Graded Hypoxia and Reoxygenation (Group A, n = 5)*

| $FIO_2$ | $Pao_2$ | $Cao_2$ | $Pvo_2$ | $Cvo_2$ | HR | Pa mean |
|---|---|---|---|---|---|---|
| % | *mmHg* | *μmol/ml* | *mmHg* | *μmol/ml* | *beats/min* | *mmHg* |
| 21 | 75.8±9.6 | 15.15±0.16 | 15.6±0.8 | 2.86±0.31 | 150±9 | 63.2±7.1 |
| 18 | 60.2±5.8* | 14.95±0.22 | 14.4±0.7 | 2.52±0.23 | 150±9 | 63.2±7.3 |
| 15 | 47.2±3.7* | 14.31±0.40* | 14.0±0.7 | 2.40±0.21 | 150±9 | 64.6±7.7 |
| 12 | 36.4±1.0* | 12.91±0.46* | 13.0±0.8* | 1.97±0.27 | 156±11 | 70.6±3.7 |
| 9 | 28.6±1.0* | 10.37±0.75* | 11.4±0.8* | 1.74±0.18* | 160±8 | 67.2±6.0 |
| 6 | 20.0±1.4* | 6.54±0.98* | 9.3±0.8* | 1.25±0.19* | 145±16 | 82.6±12.2 |
| 3 | 13.4±0.5* | 2.77±0.52* | 7.7±0.7* | 0.97±0.19* | 168±36 | 100.0±15.5 |
| 100 | 91.4±21.5 | 18.52±1.35* | 23.6±4.2 | 3.99±0.69 | 175±8 | 79.2±4.0 |
| 100 | 198.0±44.5 | 16.47±1.90 | 18.4±1.7 | 3.78±0.64 | 166±24 | 70.0±6.0 |
| 100 | 315.0±55.4* | 17.87±0.23* | 16.3±0.9 | 3.76±0.49 | 168±20 | 68.0±7.0 |
| 100 | 323.0±64.9* | 17.79±0.20* | 17.3±0.9 | 3.31±0.34 | 160±16 | 65.0±9.0 |

* $P < 0.05$ vs $FIO_2$ = 21%. Data are presented chronologically in rows representing arterial $Po_2$($Pao_2$), arterial $O_2$ content ($Cao_2$), coronary sinus $Po_2$ ($Pvo_2$), coronary sinus $O_2$ content ($vo_2$), heart rate (*HR*), and arterial mean pressure (*Pa mean*) during graded hypoxia and reoxygenation.

maintenance of oxygen consumption rate. Net lactate release terminates with reoxygenation and a return to net myocardial lactate uptake. During the graded hypoxia period circulating arterial lactate levels increased from 2.8±0.52 to 8.3±1.11 mM ($P < 0.01$), reflecting increased lactate release from other tissues as well as heart. The transition from high net lactate release to net lactate uptake occurs within the first 8 min of recovery. Glucose uptake and release were also measured. However, results of these studies were inconsistent, and no clear-cut relationship could be defined.

Typical $^{31}P$ spectra obtained from the control period are shown with peak assignments in Fig. 4. These spectra represent the sum of 60 spectra obtained within 2 min. All spectra were originally acquired in 30 s blocks. A stackplot of 30-s spectra from an individual experiment is shown in Fig. 5. A large increase in intracellular phosphate corresponds with the decrease in PCr and ATP. Maximal linebroadening applied during processing increased signal to noise in the Fourier Transform data obtained from these blocks and enabled analysis of PCr and ATP peak areas using the least squares analysis program described by Heineman and Balaban (14). A typical plot of relative peak areas obtained with 30-s resolution is exhibited in Fig. 6. In this experiment steady state PCr and ATP levels occur through $FIO_2$ 6%, followed by a rapid decline first in PCr and then in ATP during the $FIO_2$ 3% period. The PCr recovery during reoxygenation follows an exponential time course, although the initial period is linear and regression analysis is applicable for determination of PCr recovery rates (see Discussion).

Relative PCr and ATP areas obtained from the 2-min spectra are illustrated in Fig. 7. Summing of data into 2-min blocks improves signal to noise, enhances peak area analysis, and enables measurement of the PCr-Pi chemical shift required for intracellular pH ($pH_i$) determination (Fig. 8). Intracellular phosphate is higher in aerobically functioning sheep heart than in other species, and the NMR peak is uncontaminated by 2,3 diphosphoglycerate (13). The data indicate that PCr and ATP decline, while myocardial oxygen consumption is maintained and anaerobic production of lactate increases during hypoxia. Concurrently no significant change in $pH_i$ occurs. Full and rapid

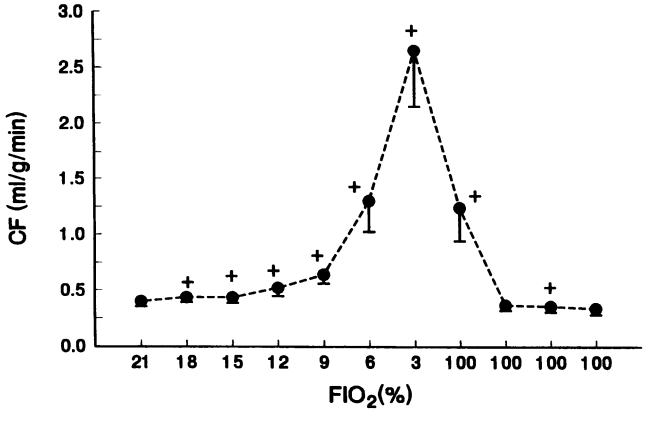


*Figure 1.* Coronary flow is plotted as a function of $FIO_2$ during graded hypoxia in sheep ($n$ = 5). Each period of hypoxia lasted for 4 min. Coronary flow values represent the mean for each period. $^+P < 0.05$ vs $FIO_2$ = 21%.

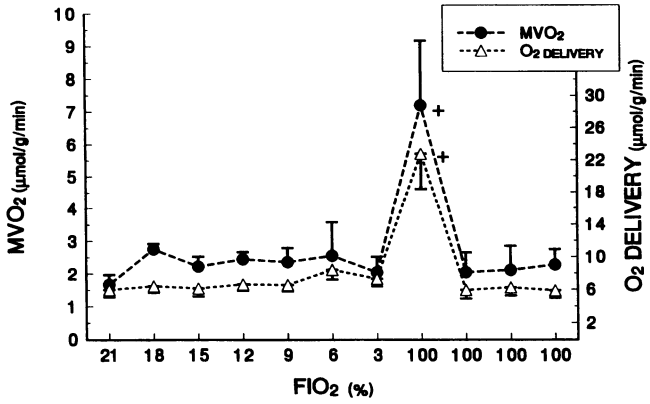


*Figure 2.* Myocardial oxygen consumption and oxygen delivery expressed a micromole per gram per min are plotted vs $FIO_2$. $^+P < 0.05$ vs $FIO_2$ = 21%.

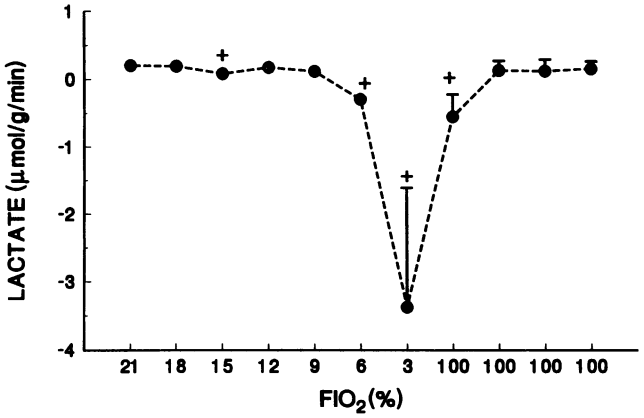


*Figure 3.* Myocardial net lactate uptake vs $FIo_2$ is plotted. Negative values indicate that net lactate release occurs. $^{+}P < 0.05$ vs $FIo_2 = 21\%$.

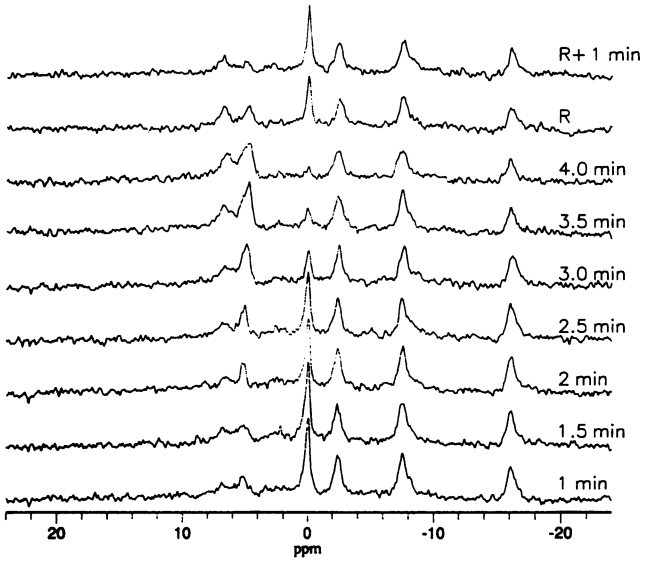


*Figure 5.* A representative stack plot of spectra (30-s blocks) during $FIo_2$ 3% and reoxygenation is illustrated. 10 Hz linebroadening is applied during processing. Spectra appear chronologically from bottom to top. Time noted at the right is the time into $FIo_2$ 3% that block acquisition was commpleted. *R* represents the first 30 s of reoxygenation. A rapid drop in phosphocreatine associated with an increase and broadening of the Pi peak continues through hypoxia. Rapid reestablishment of the phosphocreatine peak with diminution of the Pi signal occurs during reoxygenation.

PCr recovery during reoxygenation coincides with the period of increased oxygen consumption. ATP levels do not recover.

Unlike the group undergoing graded hypoxia, the animals which underwent moderate but steady state hypoxia (group B) showed no changes in PCr or ATP. $Po_2$ was maintained between 25 and 35 for 18 min. This was accompanied by a modest increase in coronary sinus flow and no change in myocardial oxygen consumption.

Hemodynamic data from the animal group, which underwent functional assessment (group C) during graded hypoxia are summarized in Table II. No decreases in $dP/dt$ or power occurred during graded hypoxia. Left ventricular power did increase during $FIo_2$ 3% and remained elevated through early reoxygenation. $dP/dt$ did increase significantly during the initial reoxygenation period. The catecholamine profiles from the group C experiments are summarized in Table III. Marked increases in circulating catecholamines occurred during the graded hypoxia protocol.

## Discussion

This examination of myocardial energetics during hypoxia was completed under the constraints inherent to studies performed in vivo. Myocardial energy metabolism was thus subjected to systemic factors such as circulating hormone levels and peripheral vasoreactivity, which are themselves responsive to hypoxia. Possibly due to these influences, contractile failure frequently noted in isolated perfused hearts during hypoxia (1, 4, 16), was not readily apparent. Although the hemodynamic responses to hypoxia are blunted in ventilated sheep (17) the degree of hyp-

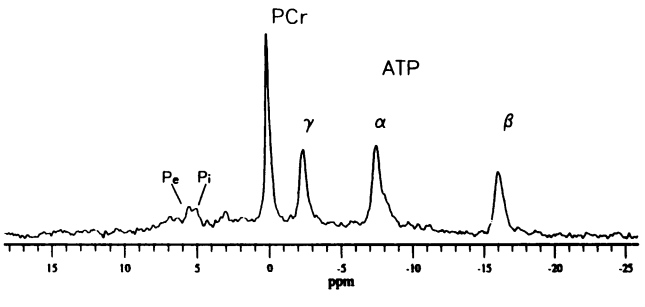


*Figure 4.* Representative 2 min $^{31}P$ spectra (60-summed acquisitions) are illustrated. Baseline correction and 5 Hz linebroadening were applied. Major peak assignments are noted: Pe, extracellular phosphate; ATP denotes three peaks of adenosine triphosphate. See Portman and Ning (reference 13) for detailed discussion of sheep heart spectra.

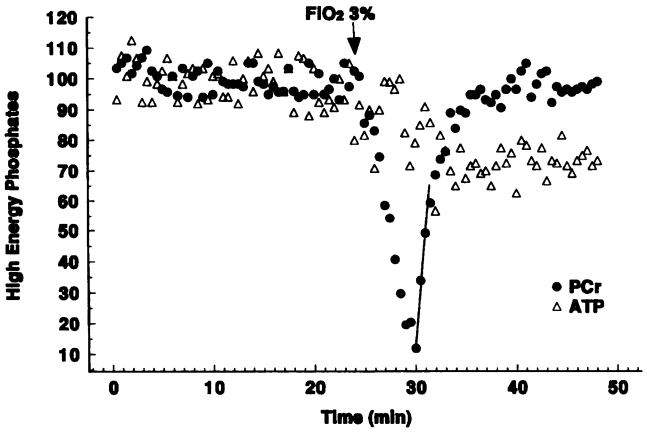


*Figure 6.* A typical plot of high energy phosphate peak areas (expressed as percentage of baseline) obtained with 30-s resolution is exhibited. Relative PCr and ATP peak areas are plotted vs time as $FIo_2$ is decreased from 21 to 3% in 3% increments every 4 min. PCr depletion during this particular experiment is extreme and begins during $FIo_2$ 3%, as indicated by the arrow. The linear PCr recovery is noted by the solid line. The slope, determined through linear regression analysis, can be used in conjunction with freeze clamp extraction data and baseline saturation corrected PCr/ATP to calculate the creatine rephosphorylation rate.

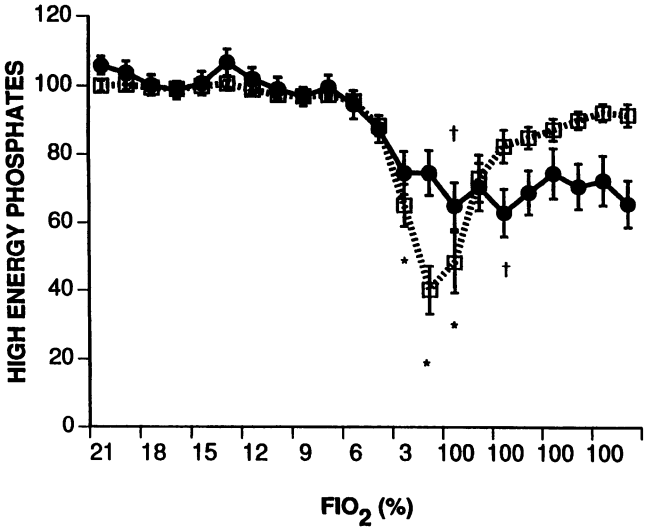


*Figure 7.* High energy phosphate peak areas (expressed as percentage of baseline) for 2-min acquisition blocks are plotted vs $FIO_2$ during graded hypoxia in sheep ($n = 5$). Significant decreases in PCr "□" do not occur until $FIO_2$ 3%. The ATP "●" does not decrease significantly until the first 2-min of reoxygenation. ATP does not recover during this protocol. * (PCr), † (ATP) $P < 0.05$ vs $FIO_2 = 21\%$.

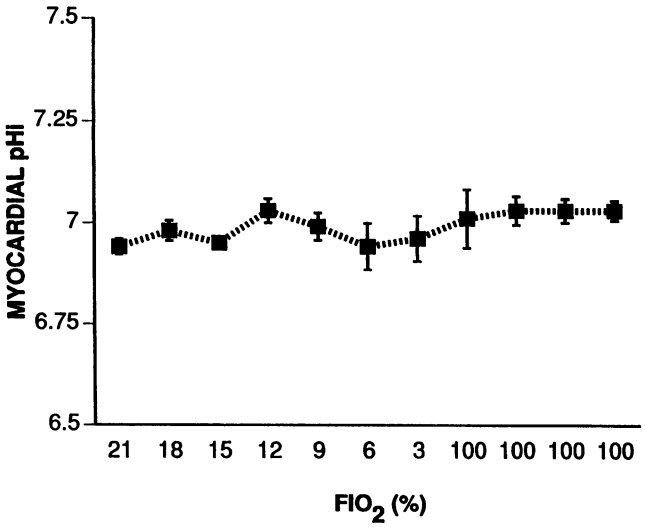


*Figure 8.* Myocardial intracellular pH and $pH_i$ are plotted vs $FIO_2$ during graded hypoxia ($n = 5$). No significant changes in $pH_i$ occurred during this protocol.

oxia was sufficient to produce rapid depletion of myocardial high energy phosphates without leading to hypotension and demise of the subject under study. Thus, although the energy metabolism during contractile failure could not be studied, measurement of myocardial reoxygenation parameters including rephosphorylation was enabled.

These experiments were conducted under the limitations imposed by an NMR surface coil, which did not use a homogenous radiofrequency field. Therefore, it is likely that subepicardial areas of the left ventricle contributed more to the signal than other regions (18). Lack of 2,3 diphosphoglycerate peaks in sheep heart phosphorous spectra does not indicate that signal is obtained primarily from epicardium. This metabolite occurs at levels which cannot be detected by $^{31}P$ magnetic resonance spectroscopy (13). The radius of the surface coil used in these experiments should limit the radiofrequency penetration to the left ventricular myocardium, but further localization information is not available. Although controversial, some heterogeneity in energy metabolism probably also exists across the left ventricular wall (19). This postulate is reinforced by $^{31}P$ NMR studies which have used homogenous radiofrequency fields in association with localization pulse sequences and found small transmural variations in PCr/ATP (20). In the present experiments relative concentrations in phosphorous metabolites summed across the sampling area were analyzed, with the understanding that specific portions of myocardium may have more or less change during hypoxia and recovery. Furthermore, these data are related to global left ventricular measurements of substrate uptake and function. These limitations should be considered when interpreting the results of this study.

Myocardial oxygen consumption was maintained throughout the hypoxia imposed during this protocol. Concomitant high energy phosphate depletion during the severest hypoxia indicates that an imbalance between ATP production and utilization exists. ATP hydrolysis exceeds synthesis through both aerobic and anaerobic pathways. Thus energy reserves are accessed primarily in the form of PCr, the primary energy buffer, but also from the cytosolic ATP pool. Estimation of high energy phosphate pool utilization which appears to be linear in the late period of hypoxia can be made from freeze clamp extraction data and initial saturation corrected PCr/ATP ratio as previously described (21). Using approximate baseline levels of 12 μmol/g PCr and 6.9 μmol/g ATP in the mature sheep (21) for estimations, then < 3.0 μmol/g per min high energy phosphate reserve was used during this period. This compares to concurrent ATP production of 13.5±1.5 μmol/g per min through oxidative phosphorylation, calculated from oxygen consumption and assuming a P:$O_2$ ratio of 5.4 (21). Furthermore up to 5 μmol ATP/g per min are likely produced through anaerobic glycolysis, estimated from concomitant lactate release, assuming that glycogen is the primary source. Summing the rates of aerobic and anaerobically produced ATP with the rate of high energy phosphate depletion reveals that ATP utilization increased an average of 59±20% during the period of severest hypoxia. Whether this represents decreased efficiency of ATP utilization or an increase in cardiac work cannot be definitively determined. However, cardiac power, an index of cardiac work, did increase between 33 and 46% during $FIO_2$ 3% in the group C studies. This corresponds with the period of rapid high energy phosphate depletion in group A, thus providing some evidence that increased demand contributes to the energy imbalance.

The degree of high energy phosphate depletion documented in this study is far greater than that found in previous studies, which have examined high energy phosphate changes during hypoxia (10, 11). Pool and associates used a rapidly frozen biopsy technique to obtain serial samples from canine hearts during hypoxia, which then underwent standard chemical analyses for PCr and ATP (10). Only small changes in PCr and no significant changes in ATP were found during those experiments. Conceivably some of those discrepancies may be related to species differences, but substantial variations in the protocols and techniques are more likely causes. Hypoxia was more moderate ($Po_2$ 30–40 mmHg) and adrenergic blockade was used to prevent catecholamine-induced augmentation of cardiac func-

*Table II. Cardiac Function Parameters for Graded Hypoxia and Reoxygenation (Group C, n = 4)*

| $FIO_2$ | $PaO_2$ | LVEDP | LVDP | dP/dt max | −dP/dt max | CO | HR | Pa mean | POWER | POWER max |
|---|---|---|---|---|---|---|---|---|---|---|
| % | *mmHg* | *mmHg* | *mmHg* | *mmHg/s* | *mmHg/s* | *liter/min* | *beats/min* | *mmHg* | *mmHg · liter/min* | *mmHg · liter/min* |
| 21 | 72.1±13.4 | 4.5±1.0 | 79.8±9.6 | 2,900±238 | 1,600±408 | 1.3±0.31 | 157.5±1.5 | 79.2±11.4 | 104.4±34.6 | 305.6±79.4 |
| 18 | 58.0±12.0* | 4.5±1.0 | 80.3±9.4 | 2,900±191 | 1,600±316 | 1.2±0.34 | 157.5±1.5 | 81.7±12.8 | 106.4±40.7 | 318.6±100.3 |
| 15 | 53.3±9.7* | 4.0±1.7 | 78.3±9.8 | 2,850±263 | 1,500±332 | 1.3±0.29 | 157.5±1.5 | 77.8±12.0 | 105.9±35.3 | 308.2±78.9 |
| 12 | 37.1±3.7* | 4.5±1.0 | 80.3±8.1 | 3,150±330 | 1,600±294 | 1.4±0.30 | 157.5±1.5 | 78.3±9.5 | 117.5±35.7 | 348.2±93.6 |
| 9 | 31.5±5.5* | 4.3±0.9 | 96.5±19.3 | 4,750±1,638 | 1,850±310 | 1.4±0.39 | 157.5±1.5 | 81.5±7.3 | 122.1±36.2 | 436.8±105.8 |
| 6 | 20.9±3.1* | 4.0±1.7 | 80.5±7.1 | 3,650±171* | 1,250±126 | 1.8±0.46 | 157.5±1.5 | 78.4±2.8 | 143.3±37.7 | 435.2±63.0* |
| 3 (2 min) | 13.0±2.3* | 14.3±6.4 | 99.0±8.0 | 4,150±287 | 2,200±141 | 2.2±0.75 | 150±12.2 | 100.7±6.1 | 208.5±58.8* | 651.4±77.3* |
| 3 (4 min) | 12.0±2.6* | 14.3±4.1* | 90.5±5.3 | 4,350±750 | 2,100±173 | 2.2±0.71 | 150±21.2 | 89.0±7.3 | 191.7±60.0* | 634.6±65.9* |
| 100 (1 min) | | 1.0±0.7* | 153.0±13.5* | 7,700±885* | 3,150±419 | 2.0±0.51 | 175±8.7 | 94.8±17.8 | 184.3±64.3* | 743.0±128.4* |
| 100 (4 min) | 199.2±114.7 | 6.5±3.0 | 81.8±10.3 | 3,100±1,139 | 1,550±310 | 1.6±0.37 | 151.5±11.0 | 76.9±8.11 | 126.1±35.1 | 457.6±192.6 |
| 100 (8 min) | 200.9±120.9 | 11.8±2.9 | 43.3±8.1 | 1,050±126* | 700±173 | 1.1±0.26 | 150.0±12.2 | 60.5±7.8 | 73.2±22.8 | 126.1±15.4 |
| 100 (12 min) | 205.6±125.7 | 11.8±2.8* | 34.3±3.4* | 850±96* | 500±129* | 0.8±0.20 | 150.0±12.2 | 52.9±5.0* | 43.54±10.42 | 100.3±28.4 |
| 100 (16 min) | 221.4±128.4 | 9.8±2.1* | 52.5±3.1* | 1,250±222* | 850±171* | 1.0±0.25 | 150.0±12.2 | 60.6±16.9 | 60.53±16.93 | 157.0±36.1 |

* $P < 0.05$ vs $FIO_2$ = 21%. Data are presented in chronological order by row. $PaO_2$, arterial $PO_2$; LVEDP, left ventricular diastolic pressure; CO, cardiac output; HR, heart rate; Pa mean, mean arterial pressure; POWER, left ventricular power.

tion. No change in high energy phosphates during similar degrees of hypoxia were noted during the present study. Osbakken and colleagues have reported decreases in myocardial PCr/ATP while arterial $PO_2$ was maintained between 20 and 30 mmHg, values which are still higher than the present nadir 13±0.5 mmHg at $FIO_2$ 3% (11). In the present study, time-dependent changes in high energy phosphates did not occur in the steady-state hypoxia group B. A critical $PO_2$ was determined by plotting individual arterial $PO_2$ values during graded hypoxia vs relative high energy phosphate concentration. Exponential curve fitting was applied and results are illustrated in Fig. 9. This analysis demonstrates that no decrease in high energy phosphates occurs until arterial $PO_2$ drops to between 17–20 mmHg during conditions provided in this study. Within this respective $PO_2$ range, myocardial respiration likely becomes dependent on cellular oxygen supply now limited by the diminished capillary to mitochondrial $O_2$ gradient (5, 22). Although the respiration rate is steady, further increases to balance the increased ATP hydrolysis rate are limited by the decreased $O_2$ gradient.

Rapid depletion of cytosolic ATP occurred during severe hypoxia. Furthermore, unlike phosphocreatine, no repletion occurred during reoxygenation. Since absolute high energy phosphate concentrations are not determined in these studies, ATP peak area relative to baseline is dependent on signal to noise ratio changes which may occur during the protocol. Alteration in signal to noise ratio might occur through variations in shim or ambient radiofrequency noise. Consistent linewidths of the $\gamma$ and $\beta$ ATP peaks through serial spectra indicate that it is unlikely that alterations in shim occurred. Furthermore full recovery of the PCr peak indicates that it is unlikely that a substantial change in the signal to noise ratio occurs. ATP depletion during severe hypoxia and brief ischemia without early repletion accompanying oxygenation is a well-documented phenomenon (23, 24). Swain and associates noted prolonged myocardial ATP depletion even after reperfusion following brief coronary occlusion in canines (23). ATP loss is generally attributed to

*Table III. Plasma Catecholamine Levels (picograms/milliliter)*

| $FIO_2$% | Sheep | Epinephrine | Norepinephrine | Dopamine |
|---|---|---|---|---|
| 21 | 1 | < 25 | 246 | < 25 |
| | 2 | < 25 | 223 | < 25 |
| | 3 | < 25 | 400 | < 25 |
| | 4 | < 25 | 453 | < 25 |
| | mean±SE | < 25 | 330±56 | < 25 |
| 21 | 1 | < 25 | 246 | < 25 |
| | 2 | < 25 | 269 | < 25 |
| | 3 | < 25 | 455 | < 25 |
| | 4 | < 25 | 341 | < 25 |
| | mean±SE | < 25 | 327±47 | < 25 |
| 3 | 1 | 30,160 | 39,460 | < 25 |
| | 2 | 33,290 | 41,140 | 152 |
| | 3 | 25,190 | 43,750 | 254 |
| | 4 | 22,500 | 22,380 | < 25 |
| | mean±SE | 27,785±4,848* | 36,682±4,848* | 114±55 |

* $P < 0.05$ vs $FIO_2$ = 21%. Individual catecholamine levels are presented for Group C sheep ($n$ = 4). Data were obtained during the initial stabilization period ($FIO_2$ 21%), just before initiating graded hypoxia ($FIO_2$ 21%), and at $FIO_2$ 3%.

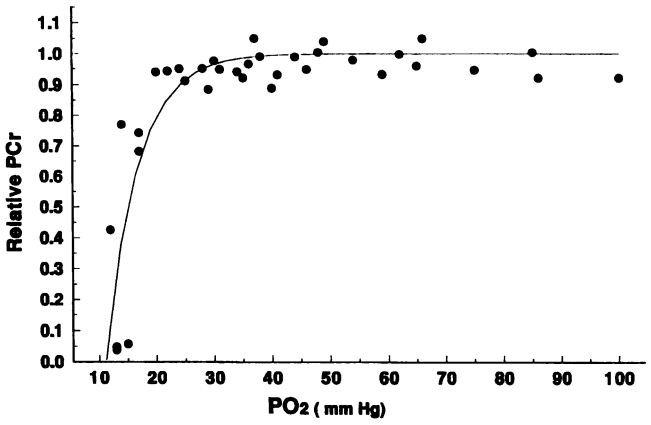


*Figure 9.* Exponential curve analysis of relative PCr vs arterial $PO_2$ in sheep ($n$ = 5) undergoing graded hypoxia.

purine degradation and loss, which may be accelerated by high coronary flow rates generated during hypoxia.

Decreases in cardiac function did not occur with the levels of hypoxia provided in these experiments. Maintenance or even slight increases in cardiac function during hypoxia are findings consistent with those published by previous investigators when employing ventilated sheep as a model (17, 25). However, dissociation of functional parameters from myocardial intracellular phosphate levels as occurred during this study is fairly specific to the particular study conditions (2, 26–28). Intracellular phosphate as well as pH have been implicated as regulators of contractile function during hypoxia or ischemia (24, 27, 29). The codependence of these factors in modulation of myocardial force generated during oxygen deprivation is a subject of controversy (30). Studies performed in perfused hearts (16), and in skinned rat ventricular myocytes (29) indicate that increases in intracellular phosphate cause a decline in maximal $Ca^{2+}$ activated force. This relationship appears to be pH independent, at least in skinned fiber studies. Separation of these parameters in perfused hearts is difficult to accomplish (16, 24). In contrast, decreases in Pi occur independently of pH, but are not associated with myocardial contractile depression in the present model studied in vivo. Previously, dissociation of cardiac function and intracellular phosphate concentration has been noted only in myocardium receiving substantial adrenergic stimulation during hypoxia or ischemia (28, 31). This has occurred during catecholamine stimulation in hypoxic buffer–perfused hearts (28), and regionally ischemic myocardium in vivo (31). Accordingly, high levels of circulating catecholamines were measured during severe hypoxia in this study.

Studies performed in ventricular skinned fibers have supported the suggestion, that Pi inhibits actomyosin cycling with a resultant decrease in crossbridge formation. This mechanism would diminish $Ca^{2+}$ activated maximal force (29, 32). Conceivably, catecholamine stimulation during hypoxia would counter such an effect by increasing $Ca^{2+}$ sarcoplasmic reticulum release and recycling, as well as possibly influencing myofibril sensitivity to $Ca^{2+}$ (33). The inotropic effect of the catecholamines would increase the rate of ATP utilization, while maintaining or, as occurred in this study, increasing contractile function.

*Rephosphorylation.* Reoxygenation of hypoxic mitochondria leads to both structural and functional mitochondrial abnormalities (34), which are often associated with respiratory uncoupling, but do not necessarily prevent eventual reestablishment of free energy level (35). Thus examination of high energy phosphate levels before and after reoxygenation is not particularly useful as an assessment of mitochondrial function during reoxygenation. Piper has recently suggested that dynamic measurements of rephosphorylation would be more effective evaluations of mitochondrial function (36), although such is technically difficult to perform in vivo.

In this study, the initial creatine rephosphorylation rate, 4.3±0.6 μmol/g per min, is calculated using the slope obtained from linear regression analysis of the first PCr recovery points obtained from the 30-s spectra for each experiment as illustrated in Fig. 6, in conjunction with freeze clamp extraction data and saturation corrected PCr/ATP as previously noted. Though creatine is rephosphorylated to baseline PCr concentration, ATP levels do not recover within the protocol period.

This measured creatine rephosphorylation rate ($\Delta PCr_{meas}$) provides an index of mitochondrial function (30). A value,

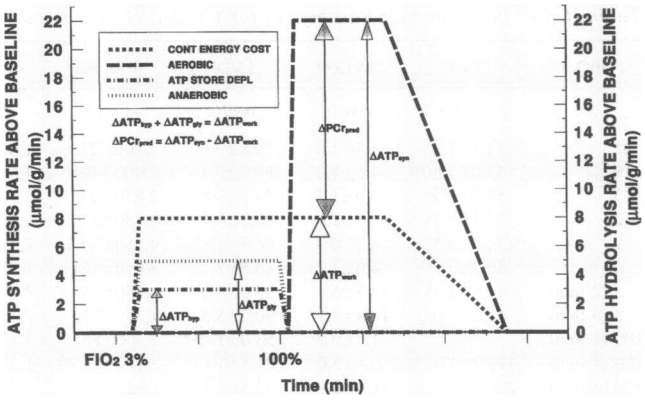


*Figure 10.* Schematic representing changes in various components of ATP synthesis and hydrolysis which facilitate calculation of the predicted creatine rephosphorylation rate ($\Delta PCr_{pred}$) during reoxygenation. All plots refer to values above baseline. Major tick marks in x-axis are 2 min intervals; $FIO_2$ in percent is also indicated along x-axis. *CONT ENERGY COST* refers to contractile energy cost measured as a rate of ATP hydrolysis. *AEROBIC* is the ATP synthesis rate through oxidative phosphorylation. *ATP STORE DEPL* is the rate of PCr and ATP store depletion. *ANAEROBIC* is the rate of anaerobic ATP synthesis. The height of each arrow indicates the value of the associated component used in calculation of $\Delta PCr_{pred}$ (see main text for the definition of components).

which is less than expected, indicates that mitochondrial damage and/or decoupling of oxidative phosphorylation occurred during reoxygenation or preceding hypoxia. The expected or predicted rephosphorylation rate must first be determined to provide a basis for comparison, and requires consideration of several components (Fig. 10). Primary among these is the increase in contractile energy cost, and thus ATP hydrolysis, which is established during hypoxia grade $FIO_2$ 3%. Initially, this rise in energy cost is compensated through anaerobic ATP synthesis as well as high energy phosphate store depletion. As cardiac work is constant (group C data) from hypoxia grade $FIO_2$ 3% through early reoxygenation, the contractile energy requirement does not change over the transition. However, during reoxygenation the raised contractile energy cost can be balanced through increased oxygen consumption and accelerated oxidative phosphorylation; while anaerobic contribution to ATP synthesis is considered negligible, since lactate release substantially decreases. Aerobic ATP synthesis, which is surplus above the contractile energy cost during reoxygenation, may be directed into creatine rephosphorylation through the forward creatine kinase reaction: creatine + ATP + H+ ⇄ PCr + ADP.

The creatine rephosphorylation rate ($\Delta PCr_{pred}$) may be predicted if the increase in contractile energy cost ($\Delta ATP_{work}$) and the increase in aerobic ATP synthesis rate ($\Delta ATP_{syn}$) during reoxygenation are known. The first component can be calculated from parameters measured during hypoxia and may be expressed mathematically as $\Delta ATP_{work} = \Delta ATP_{hyp} + \Delta ATP_{gly}$. $\Delta ATP_{hyp}$ symbolizes the energy store depletion and $\Delta ATP_{gly}$ represents the anaerobic ATP synthesis. This latter term is considered to be equivalent to 1.5 times the lactate release rate during the $FIO_2$ 3% period, while assuming the majority of this ATP is glycogen derived (37). Some overestimation of $\Delta ATP_{gly}$ likely occurs during these experiments because an increase in lactate release can result from decreased lactate

uptake as well as an increase in production. The second important component is $\Delta ATP_{syn}$, symbolizing the increase in the aerobic ATP synthesis rate during reoxygenation, and is derived through: $\Delta MVo_2 \times P:O_2$. The operative $P:O_2$ is 5.4, a value obtained from published studies of functioning sheep myocardium in vivo (see reference 21 for review of $P:O_2$ values). Use of this value employs the postulate that ATP synthesis optimally couples to oxidative phosphorylation during reoxygenation. The final calculation is $\Delta PCr_{pred} = \Delta ATP_{syn} - \Delta ATP_{work}$, and provides the final value for reference to the actual measured rephosphorylation rate. The exaggeration of anaerobic ATP production as noted above likely leads to some systematic underestimation of $\Delta PCr_{pred}$. Nevertheless, calculation of these parameters from the individual experiments reveals that $\Delta PCr_{pred}$ is $14.8 \pm 4.9$ $\mu$mol/g per min ($P < 0.05$ by paired $t$ test), and that $\Delta PCr_{meas}$ is found to be only $34 \pm 11\%$ $\Delta PCr_{pred}$.

The measured rephosphorylation rate falls well below the predicted in these experiments; this implies that energy provided through the respiratory complexes and substrate oxidation is consumed by processes other than ADP phosphorylation during reoxygenation in vivo. Respiratory uncoupling does occur consistently in isolated mitochondria and cell preparations, which have been exposed to anoxia or hypoxia and are reoxygenated or reperfused (38). Such mitochondrial dysfunction is closely linked to increased membrane permeability (39), which results in transient accumulations of mitochondrial $Ca^{2+}$ during the immediate reoxygenation period (38, 40, 41). Oxidation is then preferentially coupled to $Ca^{2+}$ transport over ATP synthesis, thus diminishing the $P:O_2$ value. Permeabilization of the mitochondrial membrane may be mediated through processes activated by inorganic phosphate, decreasing pH, and oxidative stress (38, 39, 42). Mitochondrial $Ca^{2+}$ accumulation also leads to loss of respiratory chain complexes (43) and enzymes (44), and partial depolarization of the mitochondrial membrane (40) with a reduction in membrane proton electrochemical potential (39).

The mechanism for respiratory uncoupling in myocardium in vivo is yet unclear, and it is difficult to extrapolate operative processes in myocytes and isolated mitochondria to whole tissue exposed to graded hypoxia. The diminished measured rephosphorylation rate represents an average throughout the myocardial area under study, and could reflect either partial decoupling in all cells or total irreversible decoupling in some cells with others unaffected. Furthermore, the transient nature of this abnormality cannot be verified, although excess $Ca^{2+}$ is eventually cleared from isolated mitochondria (38) and myocytes (45) and $P:O_2$ is not diminished in glycolytically inhibited perfused hearts after ischemia (46).

This study demonstrates that myocardial high energy phosphate depletion can occur during hypoxia without associated decreases in cardiac function or oxygen consumption. It is likely that catecholamine effects supersede any regulatory mechanism through Pi, which may be apparent in studies performed in isolated heart preparations. Further examination of these catecholamine effects is necessary to confirm this hypothesis. Reoxygenation in this model in vivo is accompanied by creatine rephosphorylation, which proceeds at a rate well below predicted. This indicates that mitochondrial respiratory uncoupling and possible damage occurs during reoxygenation. The mechanisms of such uncoupling have been partially defined in isolated myocytes and mitochondria, but remain to be verified in the heart in vivo.

## Acknowledgments

This work was funded by the National Heart, Lung, and Blood Institute, grant HL-476805.

## References

1. Dhalla, N. S., J. C. Yates, D. A. Walz, V. A. McDonald, and R. E. Olson. 1972. Correlation between changes in the endogenous energy stores and myocardial function due to hypoxia in the isolated perfused rat heart. *Can. J. Physiol. Pharmacol.* 50:333–345.

2. Kammermeier, H., E. Roeb, E. Jungling, and B. Meyer. 1990. Regulation of systolic force and control of free energy of ATP-hydrolysis in hypoxic hearts. *J. Mol. Cell. Cardiol.* 22:707–713.

3. Scheuer, J. 1967. Myocardial metabolism in cardiac hypoxia. *Am. J. Cardiol.* 19:385–392.

4. Lai, F., and J. Scheuer. 1975. Early changes in myocardial hypoxia: relations between mechanical function, pH and intracellular compartmental metabolites. *J. Mol. Cell. Cardiol.* 7:289–303.

5. Rumsey, W. L., C. Schlosser, E. M. Nuutinens, M. Robiolio, and D. F. Wilson. 1990. Cellular energetics and the oxygen dependence of respiration in cardiac myocytes isolated from adult rat. *J. Biol. Chem.* 265:15392–15399.

6. Noll, T., A. Koop, and H. M. Piper. 1992. Mitochondrial ATP-synthase activity in cardiomyocytes after aerobic-anaerobic metabolic transition. *Am. J. Physiol.* 262:C1297–C1303.

7. Herrmann, S. C., and E. O. Feigl. 1992. Adrenergic blockade blunts adenosine concentration and coronary vasodilation during hypoxia. *Circ. Res.* 70:1203–1216.

8. Berne, R. M., J. R. Blackmon, and T. H. Gardner. 1957. Hypoxemia and coronary blood flow. *J. Clin. Invest.* 20:1101–1106.

9. Kusachi, S., O. Nishiyama, K. Yasuhara, D. Saito, S. Haraoka, and H. Nagashima. 1982. Right and left ventricular oxygen metabolism in open-chest dogs. *Am. J. Physiol.* 243:H761–H766.

10. Pool, P. E., J. W. Covell, C. A. Chidsey, and E. Braunwald. 1966. Myocardial high energy phosphate stores in acutely induced hypoxic failure. *Circ. Res.* 19:221–229.

11. Osbakken, M., M. D. Mitchell, D. Zhang, A. Mayevsky, and B. Chance. 1991. In vivo correlation of myocardial metabolism, perfusion, and mechanical function during increased cardiac work. *Cardiovasc. Res.* 25:749–756.

12. Portman, M. A., F. W. Heineman, and R. S. Balaban. 1989. Developmental changes in the relation between phosphate metabolites and oxygen consumption in the sheep heart in vivo. *J. Clin. Invest.* 83:456–464.

13. Portman, M. A., and X.-H. Ning. 1990. Developmental adaptations in cytosolic phosphate content and pH regulation in the sheep heart in vivo. *J. Clin. Invest.* 86:1823–1828.

14. Heineman, F. W., J. Eng, B. Berkowitz, and R. S. Balaban. 1990. NMR spectral analysis of kinetic data, using natural line shapes. *Magn. Reson. Med.* 13:490–497.

15. Fisher, D. J., M. A. Heymann, and A. M. Rudolph. 1980. Myocardial oxygen and carbohydrate consumption in fetal lambs in utero and in adult sheep. *Am. J. Physiol.* 238 (*Heart Circ. Physiol. 7*):H399–H405.

16. Kusuoka, H., M. L. Weisfeldt, J. L. Zweier, W. E. Jacobus, and E. Marban. 1986. Mechanism of early contractile failure during hypoxia in intact ferret heart: evidence for modulation of maximal $Ca^{2+}$-activated force by inorganic phosphate. *Circ. Res.* 59:270–282.

17. Bernstein, D., and D. F. Teitel. 1990. Myocardial and systemic oxygenation during severe hypoxemia in ventilated lambs. *Am. J. Physiol.* 258 (*Heart Circ. Physiol. 27*):H1856–H1864.

18. Katz, L. A., J. A. Swain, M. A. Portman, and R. S. Balaban. 1988. Intracellular pH and inorganic phosphate content of heart in vivo: a $^{31}$P-NMR study. *Am. J. Physiol.* 255 (*Heart Circ. Physiol.*):H189–H196.

19. VanderVusse, G. J., T. Arts, J. F. C. Glatz, and R. S. Reneman. 1989. Transmural differences in energy metabolism of the left ventricular myocardium: fact or fiction. *J. Mol. Cell. Cardiol.* 22:23–37.

20. Robitaille, P. M., H. Merkle, B. Lew, G. Path, K. Hendrich, P. Lindstrom, A. H. From, M. Garwood, R. J. Bache, and K. Ugurbil. 1990. Transmural high energy phosphate distribution and response to alterations in workload in the normal canine myocardium as studied with spatially localized $^{31}$P NMR spectroscopy. *Magn. Reson. Med.* 16:91–116.

21. Portman, M. A. 1994. Measurement of Pi-ATP flux in lamb myocardium in vivo. *Biochim. Biophys. Acta.* 1185:221–227.

22. Wittenberg, B. A., and J. B. Wittenberg. 1985. Oxygen pressure gradients in isolated cardiac myocytes. *J. Biol. Chem.* 260:6548–6554.

23. Swain, J. L., R. L. Sabina, P. A. McHale, J. C. Greenfield, and E. W. Holmes. 1982. Prolonged myocardial nucleotide depletion after brief ischemia in the open-chest dog. *Am. J. Physiol.* 242 (*Heart Circ. Physiol. 11*):H818–H826.

24. Matherne, G. P., J. P. Headrick, S. Berr, and R. M. Berne. 1993. Metabolic

and functional responses of immature and mature rabbit hearts to hypoperfusion, ischemia and reperfusion. *Am. J. Physiol.* 264:H2141–2153.

25. Lee, J. C., K. H. Halloran, J. F. N. Taylor, and S. E. Downing. 1973. Coronary flow and myocardial metabolism in newborn lambs: effects of hypoxia and acidemia. *Am. J. Physiol.* 224:1381–1387.

26. Ambrosio, G., W. E. Jacobus, C. A. Bergman, H. F. Weisman, and L. C. Becker. 1987. Preserved high energy phosphate metabolic reserve in globally "stunned" hearts despite reduction of basal ATP content and contractility. *J. Mol. Cell. Cardiol.* 19:953–964.

27. Schaefer, S., G. C. Schwartz, J. A. Wisneski, S. D. Trocha, I. Christoph, S. K. Steinman, J. Garcia, B. M. Massie, and M. W. Weiner. 1992. Response of high-energy phosphates and lactate release during prolonged regional ischemia in vivo. *Circ. Res.* 85:342–349.

28. Kypson, J., and G. Hait. 1978. Myocardial metabolism and performance in hypoxia: effect of epinephrine. *J. Appl. Physiol.* 45:791–796.

29. Kentish, J. C. 1986. The effects of inorganic phosphate and creatine phosphate on force production in skinned muscles from rat ventricle. *J. Physiol.* 370:585–604.

30. Orchard, C. H., and J. C. Kentish. 1990. Effects of changes of pH on the contractile function of cardiac muscle. *Am. J. Physiol.* 258 (*Cell Physiol.* 27):C967–C981.

31. Schulz, R., B. D. Guth, K. Pieper, C. Martin, and G. Heusch. 1992. Recruitment of an inotropic reserve in moderately ischemic myocardium at the expense of metabolic recovery. *Cardiovasc. Res.* 70:1282–1295.

32. Schmidt-Ott, S. C., C. Bletz, C. Vahl, W. Saggau, S. Hagl, and J. C. Ruegg. 1990. Inorganic phosphate inhibits contractility and ATPase activity in skinned fibers from human myocardium. *Basic Res. Cardiol.* 85:358–366.

33. Drummond, G. I., and D. L. Severson. 1979. Cyclic nucleotides and cardiac function. *Circ. Res.* 44:145–143.

34. Ferrari, R., C. Ceconi, S. Curello, A. Cargnoni, E. Condorelli, S. Belloli, A. Albertini, and O. Visioli. 1988. Metabolic changes during post-ischaemic reperfusion. *J. Mol. Cell. Cardiol.* 20:119–133.

35. Siegmund, B., A. Koop, T. Klietz, P. Schwartz, and H. M. Piper. 1990. Sarcolemmal integrity and metabolic competence of cardiomyocytes under anoxia-reoxygenation. *Am. J. Physiol.* 258 (*Heart. Circ. Physiol.* 27):H285–H291.

36. Piper, H. M., T. Noll, and B. Siegmund. 1993. Mitochondrial function in the oxygen depleted and reoxygenated myocardial cell. *Cardiov. Res.* 28:1–15.

37. Mast, F., and G. Elzinga. 1990. Oxidative and glycolytic ATP formation of rabbit papillary muscle in oxygen and nitrogen. *Am. J. Physiol.* 258 (*Heart Circ. Physiol.* 27):H1144–H1150.

38. Ferrari, R., P. Pedersini, M. Bongrazio, G. Gaia, P. Bernocchi, F. DiLisa, and O. Visioli. 1993. Mitochondrial energy production and cation control in myocardial ischemia and reperfusion. *Basic Res. Cardiol.* 88:495–512.

39. Duchen, M. R., O. McGuiness, L. A. Brown, and M. Crompton. 1993. On the involvement of a cyclosporin A sensitive mitochondrial pore in myocardial reperfusion injury. *Cardiovasc. Res.* 27:1790–1794.

40. Silverman, H. S. 1993. Mitochondrial free calcium regulation in hypoxia and reoxygenation:relation to cellular injury. *Basic Res. Cardiol.* 88:483–494.

41. Crompton, M. 1990. The role of $Ca^{2+}$ in the function and dysfunction of heart mitochondria. *In* Calcium and the Heart. G. A. Langer, editor. Raven Press Ltd., New York. 167–198.

42. Crompton, M., H. Ellinger, and A. Costi. 1988. Inhibition of cyclosporin A of a $Ca^{2+}$-dependent pore in heart mitochondria activated by inorganic phosphate and oxidative stress. *Biochem. J.* 255:357–360.

43. Hardy, L., J. B. Clark, V. M. Darley-Usmar, D. R. Smith, and D. Stone. 1991. Reoxygenation-dependent decrease in mitochondrial NADH:CoQ (Complex I) activity in the hypoxic/reoxygenated rat heart. *Biochem. J.* 274:133–137.

44. Nishimura, M., H. Takami, M. Kaneko, S. Nakano, H. Matsuda, K. Kurosawa, T. Inoue, and K. Tagawa. 1993. Mechanism of mitochondrial enzyme leakage during reoxygenation of the rat heart. *Cardiovasc. Res.* 27:1116–1122.

45. Miyata, H., E. G. Lakatta, M. D. Stern, and H. S. Silverman. 1992. Relation of mitochondrial and cytosolic free calcium to cardiac myocyte recovery after exposure to anoxia. *Circ. Res.* 71:605–613.

46. Sako, E. Y., P. B. Kingsley-Hickman, A. H. From, J. E. Foker, and K. Ugurbil. 1988. ATP synthesis kinetics and mitochondrial function in the postischemic myocardium as studied by $^{31}P$ NMR. *J. Biol. Chem.* 262:10600–10607.